Journal of Experimental Botany, Vol. 61, No. 14, pp. 4021–4031, 2010
doi:10.1093/jxb/erq221 Advance Access publication 30 July, 2010
This paper is available online free of all access charges (see http://jxb.oxfordjournals.org/open_access.html for further details)

Journal of Experimental Botany
www.jxb.oxfordjournals.org

RESEARCH PAPER

The cytoskeleton enhances gene expression in the response to the Harpin elicitor in grapevine

Fei Qiao[1,2], Xiao-Li Chang[2,*] and Peter Nick[2]

[1] College of Horticulture, Northwest Argriculture & Forestry University, Yangling 712100, Shaanxi, PR China
[2] Institute of Botany 1, Karlsruhe Institute of Technology, Kaiserstrasse 2, D-76128 Karlsruhe, Germany

* To whom correspondence should be addressed. E-mail: chang.xiaoli@bio.uni-karlsruhe.de

Received 12 April 2010; Revised 7 June 2010; Accepted 21 June 2010

Abstract

The cytoskeleton undergoes dramatic reorganization during plant defence. This response is generally interpreted as part of the cellular repolarization establishing physical barriers against the invading pathogen. To gain insight into the functional significance of cytoskeletal responses for defence, two *Vitis* cell cultures that differ in their microtubular dynamics were used, and the cytoskeletal response to the elicitor Harpin in parallel to alkalinization of the medium as a fast response, and the activation of defence-related genes were followed. In one cell line derived from the grapevine cultivar 'Pinot Noir', microtubules contained mostly tyrosinylated α-tubulin, indicating high microtubular turnover, whereas in another cell line derived from the wild grapevine *V. rupestris*, the α-tubulin was strongly detyrosinated, indicating low microtubular turnover. The cortical microtubules were disrupted and actin filaments were bundled in both cell lines, but the responses were elevated in *V. rupestris* as compared with *V. vinifera* cv. 'Pinot Noir'. The cytoskeletal responsiveness correlated with elicitor-induced alkalinization and the expression of defence genes. Using resveratrol synthase and stilbene synthase as examples, it could be shown that pharmacological manipulation of microtubules could induce gene expression in the absence of elicitor. These findings are discussed with respect to a role for microtubules as positive regulators of defence-induced gene expression.

Key words: Actin, defence genes, elicitor, grapevine (*V. vinifera* cv. 'Pinot Noir', *V. rupestris*), Harpin, microtubules.

Introduction

The interaction of pathogens and their hosts is subject to an evolutionary race of arms, where the pathogens developed various strategies to circumvent or suppress defence responses of the host, whereas the host developed various strategies to sense and attack the invading pathogen or its effector molecules. The classical model for pathogen resistance has been the so-called gene-for-gene concept, where, on the side of the host, specific resistance genes (R genes) confer immunity to particular races of pathogens by recognition of so-called avirulence factors that are essential for the life cycle of the pathogen (for a review, see Dangl and Jones, 2001).

However, during recent years it became clear that the R gene defence has to be seen as highly specialized, derived situation that has evolved from much broader systems of defence that confer resistance to entire groups or classes of microorganisms. This non-host resistance (for reviews, see Heath, 2000; Thordal-Christensen, 2003) can be triggered by general elicitors, so-called pathogen-associated molecular patterns (PAMPs; for a review, see Nürnberger and Brunner 2002). In contrast to R gene-dependent defence, the responses to general elicitors do not always result in programmed cell death. Typical examples of general elicitors are chitin (Felix *et al.*, 1993) or bacterial flagellin (Felix *et al.*, 1999; Zipfel *et al.*, 2004). The signalling triggered by exogenous elicitors can be complemented by endogenous elicitors that are formed from the host cell wall upon hydrolytic attack of pathogen-derived enzymes (Davis *et al.*, 1984).

Cellular responses to elicitors include formation of cell wall papillae around sites of pathogen penetration. The

formation of these papillae is preceded by a reorganization of the cytoskeleton causing a redistribution of vesicle traffic and a cytoplasmic aggregation towards the penetration site (for reviews, see Takemoto and Hardham, 2004; Kobayashi and Kobayashi, 2008), and a, somewhat slower, migration of the nucleus (for a review, see Schmelzer, 2002). By localized mechanical stimulation of parsley cells, it was possible partially to mimic an attack by *Phytophthora sojae* and to induce several aspects of a non-host resistance including nuclear migration, cytoplasmic reorganization, formation of reactive oxygen species, and the induction of several defence-related genes (Gus-Mayer *et al.*, 1998). In contrast, localized application of the corresponding elicitor (pep-13) failed to induce the morphological changes, although it induced the full set of defence-related genes and the formation of reactive oxygen species. Interestingly, the elicitor completely inhibited cytoplasmic aggregation and nuclear migration in response to the mechanical stimulus. Since pep-13 induces in this system the activity of a mechanosensitive calcium channel (Zimmermann *et al.*, 1997), it seems that chemical and mechanical signalling converge during the cytoskeletal response to pathogen attack. Neither the mechanical stimulus, nor the elicitor, nor their combination was able to induce hypersensitive cell death in these experiments, leading the authors to conclude that additional chemical signals are required to obtain the complete pathogen response.

Traditionally, the role of the cytoskeleton has been seen as a response system that repartitions vesicle traffic and cytoplasmic architecture or executes pathogen-elicited programmed cell death. For instance, elicitor-induced reorganization of actin microfilaments was suggested to participate in the disintegration of the tonoplast during the hypersensitive response of BY-2 cells to the proteinaceous elicitor cryptogein (Higaki *et al.*, 2007). However, an increasing body of evidence (reviewed in Nick, 2008) suggests that the cytoskeleton plays a role in the sensing of abiotic stimuli such as mechanical perturbation. This leads to the question of whether actin filaments and microtubules, in addition to their response to pathogens and elicitors, might play a role upstream in elicitor-triggered signalling.

To address this question, a system was searched for, where both cytoskeletal and defence responses could be triggered differentially by treatment with an elicitor. Then it was possible to set up an experimental model based on two cell lines from grapevine genotypes that differed in their sensitivity to the Harpin elicitor. *Vitis vinifera* cv. 'Pinot Noir' is susceptible to pathogens such as *Plasmopara viticola* and *Erysiphe necator*, whereas *Vitis rupestris* efficiently copes with infection by these pathogens (Jürges *et al.*, 2009). The Harpin elicitor has been isolated as a powerful so-called type III effector from *Erwinia amylovora*, the bacterium that causes fire blight of Rosaceae (Wei *et al.*, 1992*a*). Since the *hrp* genes are conserved among phytopathogenic bacteria such as *Erwinia*, *Pseudomonas*, and *Xanthomonas* and were found to be essential for pathogenicity, they have been suggested to be the archetypical disease determinant of these pathogens. At the same time Harpin can trigger a hypersensitive response in non-host plants. This differential effect was ascribed to differential processing of Harpin in host versus non-host plants (Wei *et al.*, 1992*b*). In addition to tissue collapse in tobacco leaves, Harpin triggers an alkalinization of the apoplastic pH. Due to its broadband efficacy as a trigger of plant defence, Harpin was later commercialized under the brand name Messenger®. So far, at least to our knowledge, there are no reports of type III effectors targeting plant cytoskeletal elements.

Here it is shown that the two cell lines differ with respect to the elicitor response of microtubules and actin filaments, and that this differential response is correlated with differential microtubule stability, and a differential response of defence genes. Further, defence genes can be partially triggered by pharmacological manipulation of microtubules in the absence of elicitor, providing the first evidence for a role for the cytoskeleton as a positive regulator of elicitor-triggered gene expression.

Materials and methods

Cell lines and treatments

Suspension cell cultures of *V. rupestris* and *V. vinifera* cv. 'Pinot Noir' generated from leaves (Seibicke, 2002) were used in this experiment. They were cultivated in liquid medium containing 4.3 g l^{-1} Murashige and Skoog salts (Duchefa, Haarlem, The Netherlands), 30 g l^{-1} sucrose, 200 mg l^{-1} KH_2PO_4, 100 mg l^{-1} inositol, 1 mg l^{-1} thiamine, and 0.2 mg l^{-1} 2,4-dichlorophenoxyacetic acid (2,4-D), pH 5.8. Cells were subcultured weekly, inoculating 8–10 ml of stationary cells into 30 ml of fresh medium in 100 ml Erlenmeyer flasks. The cell suspensions were incubated at 25 °C in the dark on an orbital shaker (KS250 basic, IKA Labortechnik, Staufen, Germany) at 150 rpm. To induce cellular responses, the cultures were treated with different concentrations of a commercially available Harpin elicitor [Messenger®, EDEN Bioscience Corporation, Washington, USA; active ingredient: 3% (w/w) Harpin protein].

Measurement and quantitative analysis of pH responses

pH changes were followed by a pH meter (Schott handylab, pH 12) connected to a pH electrode (Mettler Toledo, LoT403-M8-S7/120) and recorded by a paperless record (VR06; MF Instuments GmbH, Albstadt-Truchtelfingen, Germany) at 1 s intervals. Before treatments, 2 ml of suspension cells (3–4 d after subcultivation) were pre-adapted on an orbital shaker for ~90 min until the pH was stable. To inhibit putative stretch-activated channels (Suppementary Fig. S2 available at *JXB* online), cells were pre-incubated for 30 min with water or different concentrations of $GdCl_3$ before addition of 9 µg ml^{-1} Harpin.

The pH data were exported to Microsoft Office Excel by data acquisiton software Observer II_V2.35 (MF Instruments GmbH). The data were fitted based on a Michaelis–Menten equation with $1/T_{pH50}$ as V_{max}, EC_{25} as K_m, and the concentration of Harpin as [S]. T_{pH50} was the time required to reach 50% of the maximal pH response. Due to the asymptotic behaviour of 1/T over [S], the T_{pH50} was a more reliable measure. Consequently, the equation yielded K_m as an estimate for the concentration causing 25% of the maximal response (EC_{25}).

Visualization and quantification of microtubule responses

Microtubules were visualized by indirect immunofluorescence using a monoclonal antibody against α-tubulin (DM1A; Sigma,

Taufkirchen, Germany), and a secondary anti-mouse IgG antibody conjugated to fluorescein isothiocyanate (FITC; Sigma) as described in Eggenberger *et al.* (2007). In brief, cells were fixed in customized micro-staining chambers (Nick *et al.* 2000) for 30 min with 3.7% (w/v) paraformaldehyde in microtubule-stabilizing buffer (MSB: 50 mM PIPES, 2 mM EGTA, 2 mM $MgSO_4$, 0.1% Triton X-100, pH 6.9), and then washed in MSB three times for 5 min. Subsequently, the cell wall was digested using 1% (w/v) Macerozym (Duchefa, Haarlem, The Netherlands) and 0.2% (w/v) Pectolyase (Fluka, Taufkirchen, Germany) in MSB for 5 min. To stop the digestion, the enzymes were washed out for 5 min with phosphate-buffered saline (PBS), and unspecific binding sites blocked for 30 min with 0.5% (w/v) bovine serum albumin diluted in PBS. Directly after blocking, the cells were transferred into a 1:250 dilution of the primary antibody for 1 h at 37 °C in a moist chamber. To remove unbound primary antibody, the cells were washed three times for 5 min in PBS. Then, the sample was incubated with a secondary FITC-conjugated antibody for 1 h at 37 °C in a moist chamber. Unbound secondary antibody was removed by washing with PBS. Cells were then washed three times for 5 min in PBS and observed immediately under a confocal laser scanning microscope (TCS SP1; Leica, Bensheim, Germany) using the fixed-stage configuration of the confocal laser scanning microscope with excitation by the 488 nm laser line of the ArKr laser and a four-frame averaging protocol.

Microtubule integrity was quantified from geometrical projections of complete z-stacks as described in Abdrakhamanova *et al.* (2003). After transformation into binary images to eliminate differences in overall intensity, the images were filtered using the Find Edge algorithm. The result was an image where a profile across each microtubule yielded the same integrated density, irrespective of the thickness of the microtubule or its original fluorescence intensity. Under these conditions, it was possible to obtain a linear function between integrated density along a line intersecting the microtubule array, perpendicular to the orientation of individual microtubules, and the number of microtubules intersected by this line (see Fig. 2E). This function was used to calibrate the sample data. To obtain the sample data, a lattice of five equally spaced parallel lines, 8 pixels thick, was laid over each individual cell, so that the lines were oriented perpendicular to the microtubule array and did not touch the cell wall. The integrated density along each line was then determined with the Analyze algorithm, averaged for each cell, and corrected for background measurements obtained from the same image. Microtubule frequency (defined as the number of microtubules that are intersected by a line 100 μm long) was calculated from these density values, by means of the calibration function.

Visualization of actin microfilaments

Actin microfilaments were visualized as described in Maisch and Nick (2007) with minor modifications. Suspended cells were fixed for 30 min in 1.8% (w/v) fresh paraformaldehyde in standard buffer (0.1 M PIPES, pH 7.0, supplemented with 5 mM $MgCl_2$ and 10 mM EGTA) containing 1% (v/v) glycerol and 0.1% (v/v) Triton X-100; cells were then rinsed three times for 5 min with standard buffer. Then, 0.5 ml of the resuspended cells was incubated for 30 min with 0.5 ml of 0.66 μM FITC–phalloidin (Sigma-Aldrich) freshly prepared from a 6.6 μM stock solution in 96% (w/v) ethanol by dilution (1:10, v/v) with PBS (0.15 M NaCl, 2.7 mM KCl, 1.2 mM KH_2PO_4, and 6.5 mM Na_2HPO_4, pH 7.2). Cells were then washed three times for 5 min in PBS and observed immediately by confocal laser scanning microscopy as described above.

Measuring the expression of defence-related genes

A small volume (1.5 ml) of cells was induced 5 d after subcultivation with 9 μg ml^{-1} Harpin for 0.5, 2, 4, or 6 h, or with water as negative control, sedimented by low-speed centrifugation (3000 rpm; 1 min), and shock-frozen in liquid nitrogen. Samples were homogenized with a Tissue Lyser (Qiagen/Retsch®, Germany). Total RNA was extracted from *V. rupestris* and *V. vinifera* cv. 'Pinot Noir' cells using the RNeasy Plant Mini Kit (Qiagen, Hildesheim, Germany) or the Spectrum™ Plant Total RNA Kit (Sigma) following the protocol of the producer. The extracted RNA was treated with a DNA-free DNase (Qiagen, Hildesheim, Germany) to remove potential contamination of genomic DNA. The mRNA was transcribed into cDNA using the M-MLV RTase cDNA Synthesis Kit (New England BioLabs; Frankfurt am Main, Germany) according to the manufacturer's instructions. The RNaseOUT™ RNase inhibitor (Invitrogen, Karlsruhe, Germany) was used to remove contamination by non-transcribed RNA. Transcripts were amplified by PCR primers (Table 1) with 30 cycles of 30 s denaturation at 94 °C, 30 s annealing at 60 °C, and 1 min synthesis at 72 °C. The PCR products were separated by conventional agarose gel electrophoresis after visualization with

Table 1. Designations, sequences, and literature references for the oligonucleotide primers used to amplify the marker sequences used in this study

Name	GenBank accession no.	Primer sequence 5′–3′	Reference
EF1-α	EC959059	Sense: 5′-GAACTGGGTGCTTGATAGGC-3′	Reid *et al.* (2006)
		Antisense: 5′-AACCAAAATATCCGGAGTAAAAGA-3′	
PAL	X75967	Sense: 5′-TGCTGACTGGTGAAAAGGTG-3′	
		Antisense: 5′-CGTTCCAAGCACTGAGACAA-3′	Belhadj *et al.* (2008)
CHI	X75963	Sense: 5′-GTTCAGGTCGAGAACGTCC-3′	Kortekamp (2006)
		Antisense: 5′-GCTTGCCGATGATGGACTC-3′	
CHS	AB066274	Sense: 5′-GGTGCTCCACAGTGTGTCTACT-3′	Belhadj *et al.* (2008)
		Antisense: 5′-TACCAACAAGAGAAGGGGAAAA-3′	
PR10	AJ291705	Sense: 5′-CTTACGAGAGTGAGGTCACTTC-3′	Kortekamp (2006)
		Antisense: 5′-GCAATAGAACATCACAAATACTCC-3′	
PGIP	AF05093	Sense: 5′-GATGGTACTGCGTCGAATG-3′	Kortekamp (2006)
		Antisense: 5′-GTGGAGCACCACACAAGC-3′	
RS	AF274281	Sense: 5′-GAAACGCTCAACGTGCCAAGG-3′	Kortekamp (2006)
		Antisense: 5′-GTAACCATAGGAATGCTATGTAGC-3′	
StSy	X76892	Sense: 5′-GGATCAATGGCTTCAGTCGAG-3′	Kortekamp (2006)
		Antisense: 5′-GTCACCATAGGAATGCTATGC-3′	

PR10, pathogenesis-related proteins 10, respectively; PGIP, polygalacturonase-inhibiting protein; PAL1, phenylalanine ammonia lyase 1; CHS, chalcone synthase; RS, resveratrol synthase; StSy, stilbene synthase; CHI, chalcone isomerase.

CybrSafe (Invitrogen). Images of the gels were recorded on a MITSUBISHI P91D screen (Invitrogen) using a digital image acquisition system (SafeImage™, Intas, Germany).

The bands of the products were quantified using the Image J software (http://rsbweb.nih.gov/ij/) and standardized relative to elongation factor 1α as internal standard. The results were plotted as fold increase of transcript abundance as compared with the untreated control. To test the effect of cytoskeletal drugs on Harpin-induced gene expression, cells were pre-treated for 30 min with cytoskeleton drugs including phalloidin (Sigma; 1 μM), latrunculin B (Sigma; 1 μM), oryzalin (10 μM), taxol (Fluka, Buchs, Switzerland; 10 μM), and cytochalasin D (Sigma; 5 μM), with dimethylsulphoxide (DMSO; Sigma) as solvent control [final concentration 1% (v/v) as used in oryzalin treatment], and water as negative control. After pre-treatment, cells were induced with Harpin as described above and mRNA was extracted 1 h after addition of the elicitor. The data from the quantification represent the mean from at least three independent experimental series.

Protein extraction and western blot analysis

Proteins were extracted and probed as described in Jovanović *et al.* (2010) and Nick *et al.* (1995), with minor modifications. Protein extracts were prepared from 5-day-old grapevine cells after 16 h of treatment with 9 μg ml^{-1} Harpin. After sedimentation in 15 ml test tubes (10 min, 1500 *g*; Hettich Centrifuge Typ1300, Tuttlingen, Germany), cells were homogenized in the same volume of pre-cooled 0 °C extraction buffer, containing 25 mM MES, 5 mM EGTA, 5 mM $MgCl_2$, 1 M glycerol, pH 6.9, supplemented with 1 mM dithiothreitol (DTT) and 1 mM phenylmethylsulphonyl fluoride (PMSF) by using a glass potter grinder on ice. Insoluble tissue debris was removed by centrifugation (5 min at 13 000 *g*; Heraeus Instruments, Biofugepico, Osterode, Germany, rotor PP1/96 #3324), followed by ultracentrifugation (15 min at 100 000 *g*, 4 °C; Beckman, München, Germany, TL-100, rotor TLA100.2). Proteins in the supernatant were concentrated and sedimented by precipitation with trichloracetic acid. Then the protein precipitates were washed with 80% acetone at –20 °C (vortex) and the supernatant was discarded after centrifugation (30 min at 13 000 *g*). Samples were dissolved in 200 μl of sample buffer, denatured for 10 min at 95 °C, loaded onto a standard 10% SDS–mini gel, and subjected to Western blotting as described in Nick *et al.* (1995). A pre-stained broad range protein marker (P7708S, New England Biolabs) was used as a molecular weight standard. For detection of tyrosinated α-tubulin, the monoclonal antibody ATT (Sigma-Aldrich), and for the detection of detyrosinated α-tubulin, monoclonal antibody DM1A (Sigma-Aldrich) were used at a dilution of 1:400 in TRIS-buffered saline containing Triton X-100 (TBST; 20 mM TRIS-HCl, 150 mM NaCl, 1% Triton, pH 7.4), respectively. The signal was visualized by a secondary goat anti-mouse IgA, conjugated with alkaline phosphatase (Sigma-Aldrich) at a dilution of 1:2500 in TBST with 3% (w/v) low-fat milk powder. A parallel set of lanes loaded in exactly the same manner was visualized by staining with Coomassie Brillant Blue (CBB) as a loading control.

Results

Harpin induces extracellular alkalinization

To monitor potential differences in the response of the two cell lines to the Harpin elicitor, extracellular alkalinization was used as the indicator (Fig. 1). In both cell lines, the pH increased rapidly and culminated ~30 min after addition of the elicitor, and subsequently decreased. However, in cv. 'Pinot Noir', the peak of the response was reached later (~30 min) as compared with *V. rupestris* (after 20 min).

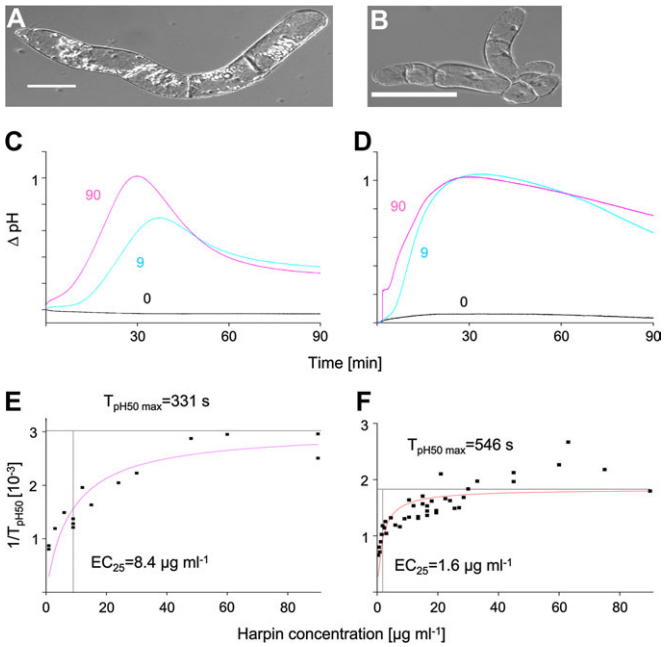

Fig. 1. Cell morphology and response of pH to Harpin in cv. 'Pinot Noir' (A, C, E) and *V. rupestris* (B, D, F). (A, B) Cell morphology in differential interference contrast. Size bar 50 μm. (C, D) Representative time courses of the pH response to 0, 9, and 90 μg ml^{-1} Harpin. (E, F) Cumulative analysis of time courses in responses to increasing concentrations of Harpin. The data were fitted using a Michaelis–Menten function. TpH_{50} represents the time to reach 50% of the maximal response. The curves represent the average from $n \geqslant 15$ individual time courses.

For cv. 'Pinot Noir', the response was accelerated and reached a higher amplitude when the concentration of Harpin was increased from 9 μg ml^{-1} to 90 μg ml^{-1} (Fig. 1C); however, in *V. rupestris*, there were no significant differences between the two concentrations (Fig. 1D). To characterize the difference between the two cell lines on a quantitative level, time courses were recorded by varying the concentration of the elicitor. The results were fitted using a Michaelis–Menten equation with pH max_{50} (the time when the pH response reached the half-maximum) as the indicator of velocity. When $1/T_{pH50}$ was plotted over the concentration of Harpin (Fig. 1E, F), saturable curves were found that fitted the Michaelis–Menten function well (R^2=0.805 for cv. 'Pinot Noir', and R^2=0.600 for *V. rupestris*). From these functions, effective concentrations (EC_{25}, inducing 25% of the maximal response) could be calculated to be 8.14 μg ml^{-1} for cv. 'Pinot Noir' and 1.65 μg ml^{-1} for *V. rupestris*, respectively. This means that the responsiveness of *V. rupestris* is roughly five times higher compared with cv. 'Pinot Noir'. To test whether putative stretch-activated channels are involved in the alkalinization response, cells were pre-incubated for 30 min with water or different concentrations of $GdCl_3$ before addition of 9 μg ml^{-1} Harpin (Supplementary Fig. S2 at *JXB* online). It was observed that, in cv. 'Pinot Noir', the peak of the response was progressively reduced from

20 μM $GdCl_3$, whereas in *V. rupestris* the pH response persisted even to 1 mM $GdCl_3$.

Harpin induces microtubule disintegration

To visualize the response of microtubules to Harpin, immunofluorescence was combined with confocal microscopy. In control cells the microtubular network was organized in arrays of parallel bundles (Fig. 2A, C). In contrast, microtubules disintegrated after addition of 9 μg ml^{-1} Harpin (Fig. 2B, D). This response was more pronounced in *V. rupestris* as compared with cv. 'Pinot Noir' (Fig. 2D). This disintegration was significant already from 1 h after addition of the elicitor (data not shown), and was completed at 3 h (Fig. 2A–D). Since the degree of Harpin-induced microtubule disintegration varied between the two *Vitis* species, microtubule integrity was quantified as described in Abdrakhamanova *et al.* (2003). As a measure of integrity, the number of microtubules intersecting a probing line perpendicular to the microtubule array was scored (Fig. 2E). Under control conditions, microtubule integrity was comparable between the two cell lines. However, in response to the elicitor, a differential behaviour became manifest. Microtubule integrity did not change significantly in the cv. 'Pinot Noir', although microtubules became finer after Harpin treatment (Fig. 2A, C). In contrast, in *V. rupestris*, microtubule frequency dropped significantly (Fig. 2F). To test whether the difference in the microtubular response is related to a difference in microtubular dynamics, the relationship between tyrosinylated versus detyrosinated α-tubulin was assessed by western blotting (Fig. 2G). Detyrosination is stimulated with increasing lifetime of microtubules and therefore can be used to monitor global microtubule turnover. The relative abundance of tyrosinylated α-tubulin (recorded by the ATT antibody) versus detyrosinated α-tubulin (recorded by the DM1A antibody) was generally elevated in cv. 'Pinot Noir' over *V. rupestris* and even increased slightly in response to the elicitor. In contrast, detyrosinated tubulin, which was hardly detectable in cv. 'Pinot Noir', was constitutively elevated in *V. rupestris*. This indicates that microtubules in cv. 'Pinot Noir' are generally endowed with a higher turnover as compared with *V. rupestris*. This is supported by the observation that growth of cv. 'Pinot Noir' is significantly more sensitive to oryzalin as compared with *V. rupestris* (Supplementary Fig. S1 at *JXB* online). Oryzalin sequesters tubulin heterodimers and eliminates microtubules depending on the level of their innate turnover.

Harpin induces actin bundling

Since the resistance of plant cells to penetration by a pathogen has been shown to depend on actin organization (Kobayashi *et al.*, 1997; for a review, see Schmelzer, 2002), the response of actin filaments to Harpin was assessed in the two cell lines. Actin filaments were visualized by fluorescent phalloidin in combination with mild fixation after 3 h incubation with 9 μg ml^{-1} Harpin. In the absence of Harpin, transvacuolar actin filaments reach from the nucleus into the cell periphery and spread into a cortial actin array in both cell lines (Fig. 3A, C). In contrast, at 3 h after addition of Harpin, the cortical actin array had significantly faded, and the finer transvacuolar actin filaments had been replaced by bundles that converge to the nucleus (Fig. 3B, D).

Harpin induces defence-related genes

To estimate expression of defence-related genes in the two cell lines, suspension cells were challenged with 9 μg ml^{-1} Harpin, and mRNA was isolated at different time points after induction (0, 0.5, 2, 4, and 6 h). The expression of defence-related candidate genes was followed by reverse transcription-PCR (RT-PCR) using the elongation factor 1α gene as internal reference for quantification. Genes involved in the phenylpropane pathway such as phenylalanine ammonia lyase (PAL), chalcone synthase (CHS), chalcone isomerase (CHI), stilbene synthase (StSy), and resveratrol synthase (RS) were used (Fig. 4A), and complemented by the pathogenesis-related protein PR10, and the polygalacturonase-inhibiting protein PGIP. Transcripts corresponding to the genes RS, StSy, and PAL accumulated transiently in both cell lines. However, the response initiated earlier and reached a higher amplitude in *V. rupestris* as compared with cv. 'Pinot Noir'. CHS and CHI were constitutively up-regulated in *V. rupestris* as compared with cv. 'Pinot Noir'. The expression of PR10 and PGIP was regulated with respect to the phenylpropane enzymes, with a stronger and earlier induction in *V. rupestris* as compared with cv. 'Pinot Noir'. Interestingly, the expression of StSy and RS that catalyse the same biochemical reaction during the biosythsis of resveratrol differs quantitatively, with a much stronger response of the StSy gene (~5-fold as compared with RS). Nevertheless, for both genes, the response was much more pronounced in *V. rupestris* than in cv. 'Pinot Noir' (Fig. 4C).

Cytoskeletal compounds induce RS and StSy in the absence of elicitor

To test whether manipulation of the cytoskeleton can mimic the effects of Harpin on the expression of defence genes, both cell lines were incubated for 30 min with compounds targeted either to actin filaments (phalloidin, latrunculin B, and cytochalasin D) or to microtubules (oryzalin and taxol). After 30 min, to one set of samples, 9 μg ml^{-1} Harpin were added and gene expression was assayed 2 h later at the time of the maximum response, whereas in the other set of samples the cells were not challenged by the elicitor. In the elicitor-treated set the expression of RS and StSy was not significantly different between the drug-treated samples, showing that the compounds did not impair the ability of the cells to respond to the elicitor. Interestingly, there was a partial (up to a third of the maximal response) but clear induction of RS and StSy in the absence of the elicitor. Similar to the previous experiments, the induction was generally more pronounced in *V. rupestris* compared with cv. 'Pinot Noir', and clearer for StSy compared with RS.

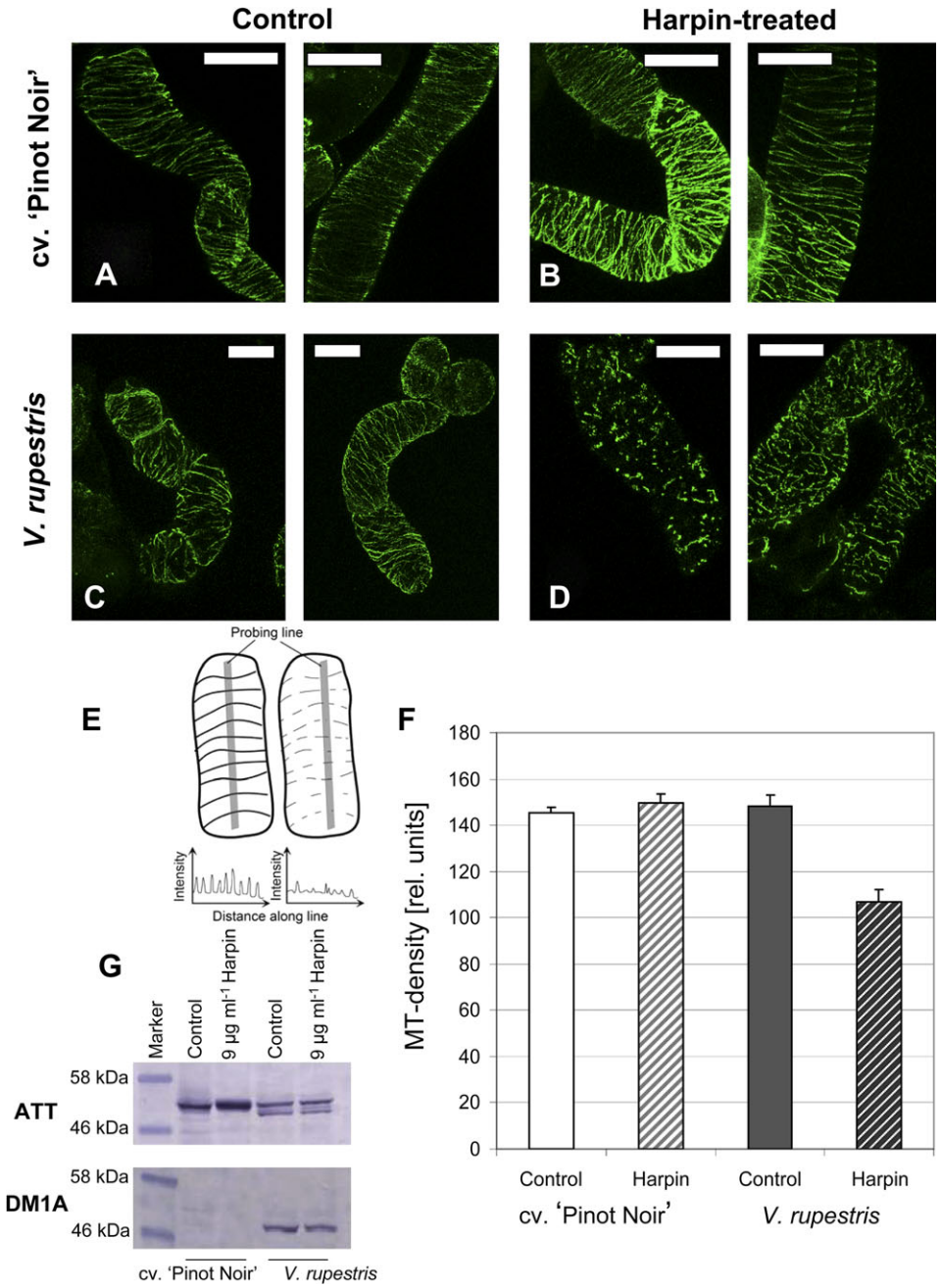

Fig. 2. Response of cortical microtubules to Harpin in cv. 'Pinot Noir' (A, B) and *V. rupestris* (C, D). Representative geometrical projections from z-stacks collected prior to (A, C) or after 3 h (B, D) of treatment with 9 μg ml^{-1} Harpin. Microtubules were visualized by immunofluorescence. Size bar=50 μm. (E) Method to quantify microtubule density (as a measure of microtubule integrity) as integrated fluorescence along a probing line. (F) Microtubule density in relative units prior to (open bars) or after 3 h of treatment with 9 μg ml^{-1} Harpin (striped bars). Error bars represent standard errors. The values summarize the data of 18–39 individual cells collected from at least three independent experiments. (G) Relative abundance of tyrosinylated α-tubulin (recorded by the ATT antibody) versus detyrosinated α-tubulin (recorded by the DM1A antibody) in total extracts from cv. 'Pinot Noir' or *V. rupestris* that had been either raised under control conditions or challenged for 16 h with 9 μg ml^{-1} Harpin. The same amount of total protein was loaded in each lane.

Independently of these differences, a consistent pattern emerged, with the strongest induction achieved by oryzalin. Taxol produced a similar, but somewhat weaker, induction, indicating that it is not only the mere presence of microtubules, but also their turnover that regulates the expression of these defence genes. Pharmacological manipulation of actin yielded weaker effects that were barely significant—if at all there was a tendency for induction in *V. rupestris* by

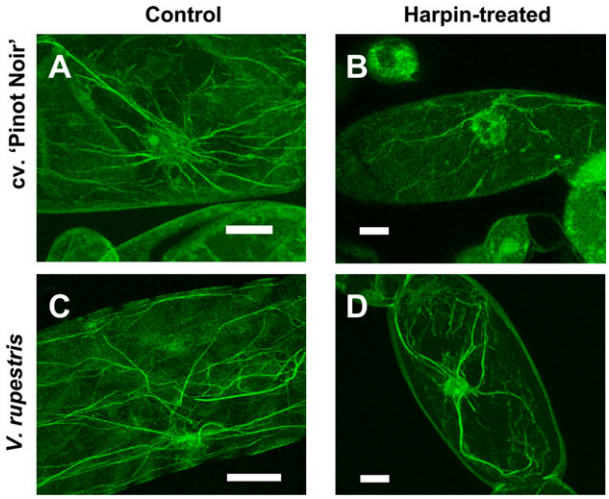

Fig. 3. Response of actin filaments to Harpin in cv. 'Pinot Noir' (A, B) and *V. rupestris* (C, D). Representative geometrical projections from z-stacks collected prior to (A, C) or after 3 h (B, D) of treatment with 9 μg ml^{-1} Harpin. Actin filaments were visualized by fluorescence-labelled phalloidin. Size bar=20 μm.

latrunculin B, a drug that very efficiently eliminates actin filaments.

Discussion

Life is not easy—this is especially true for plant cells that cannot run away, but have to cope with environmental challenges by adaptation. Pathogen defence represents a specific aspect of this general ability. Whereas the description of plant defence had been dominated by the gene-for-gene concept, during recent years evolutionarily more ancient systems of innate immunity have received attention. When a plant cell is challenged by a pathogen, it responds on two levels: biochemically, by an induction of defence genes leading to the synthesis of specific secondary metabolites with antibiotic activities, the phytoalexins (for a review, see Zhao *et al.*, 2005), and, structurally, by a repolarization of cytoplasmic architecture towards the site of penetration (for a review, see Schmelzer, 2002). These responses are triggered, for instance, by the binding of PAMPs, such as bacterial flagellin (Zipfel *et al.*, 2004), to leucine-rich repeat receptor-like kinases (for a review, see Morris and Walker, 2003). The activation of the receptor, as a next step, seems to activate ion channels, with some evidence for cross-talk with mechanosensing (Zimmermann *et al.*, 1997; Gus-Mayer *et al.*, 1998). These ion fluxes are accompanied by the formation of reactive oxygen species (Nürnberger *et al.*, 1994; Jabs *et al.*, 1996), the induction of phytoalexin metabolism, and, in some cases, programmed cell death (for a review, see Jones, 2001).

Cytoskeletal reorganization has been identified as an important element of defence responses during innate immunity and is generally interpreted as a downstream event in the context of redistributing vesicles containing phytoalexins and cell wall components towards the penetration site (for reviews, see Schmelzer, 2002; Takemoto and Hardham, 2004; Kobayashi and Kobayashi, 2008). To address the question of whether the cytoskeleton, in addition, participates in signal processing, the response to the Harpin elicitor was followed in two cell lines from grapevine genotypes that differed in their microtubule dynamics.

To monitor rapid elicitor responses upstream of gene expression, proton influx was used. Although the biological function of this proton influx is not understood, the resulting alkalinization of the external medium can be used as a simple readout for quantitative analysis of the cellular response to elicitors (Felix *et al.*, 1993), and has been employed successfully to investigate the function of Harpin (Wei *et al.*, 1992*a*). As markers for defence-related gene induction, StSy and RS were used. Stilbenes, in general, and resveratrol, in particular, have been shown to harbour antifungal activities. In fact, overexpression of StSy genes in tobacco (Hain *et al.*, 1993), rice (Stark-Lorenzen *et al.*, 1997), kiwi (Kobayashi *et al.*, 2000), alfalfa (Hipskind and Paiva, 2000), barley (Leckband and Lörz, 1998), a grapevine rootstock (Coutos-Thévenot *et al.* 2001), and apple (Szankowski *et al.*, 2003) was found to confer resistance to fungal pathogens.

Both readouts for the elicitor response showed a more sensitive and a more pronounced response of the *V. rupestris* cell line as compared with cv. 'Pinot Noir' (Figs 1, 4). This was correlated with a more pronounced response of both microtubule fragmentation (Fig. 2) and actin bundling (Fig. 3). It should be noted, however, that the cytoskeletal changes required a relatively long time to become detectable. This is certainly a drawback of the methodology used for visualization relying on fixed cells such that only relatively drastic bulk changes can be tracked. The data from pharmacological manipulation of microtubules, where defence genes could be partially induced in the absence of elicitor, indicate that microtubular responses that are much more rapid and subtle are relevant for signalling (Fig. 4D).

The microtubular disintegration was more pronounced in *V. rupestris* as compared with cv. 'Pinot Noir' in response to Harpin, although the higher abundance of detyrosinated α-tubulin (Fig. 2F) and the increased tolerance to oryzalin (Supplementary Fig. S1 at *JXB* online) indicates that microtubular lifetimes are increased in *V. rupestris*. Disintegration of microtubules can occur by different, independent mechanisms. Most 'microtubule-disrupting' drugs (this term, although often used, is in fact quite misleading) act by sequestering tubulin heterodimers such that they cannot be integrated into the growing plus end, and the microtubule disappears depending on its innate turnover. However, there exist alternative mechanisms that involve true 'disruption' of polymerized microtubules. Such microtubule disruption can be produced, for instance, by so-called severing proteins such as plant katanin (Stoppin-Mellet *et al.*, 2008). Interestingly, the microtubule-severing activity of *Shigella* (also employing a type III effector) has been found to be crucial for intercellular spreading of this pathogen (Yoshida *et al.*, 2006), and the host response to *Xanthomonas* type III

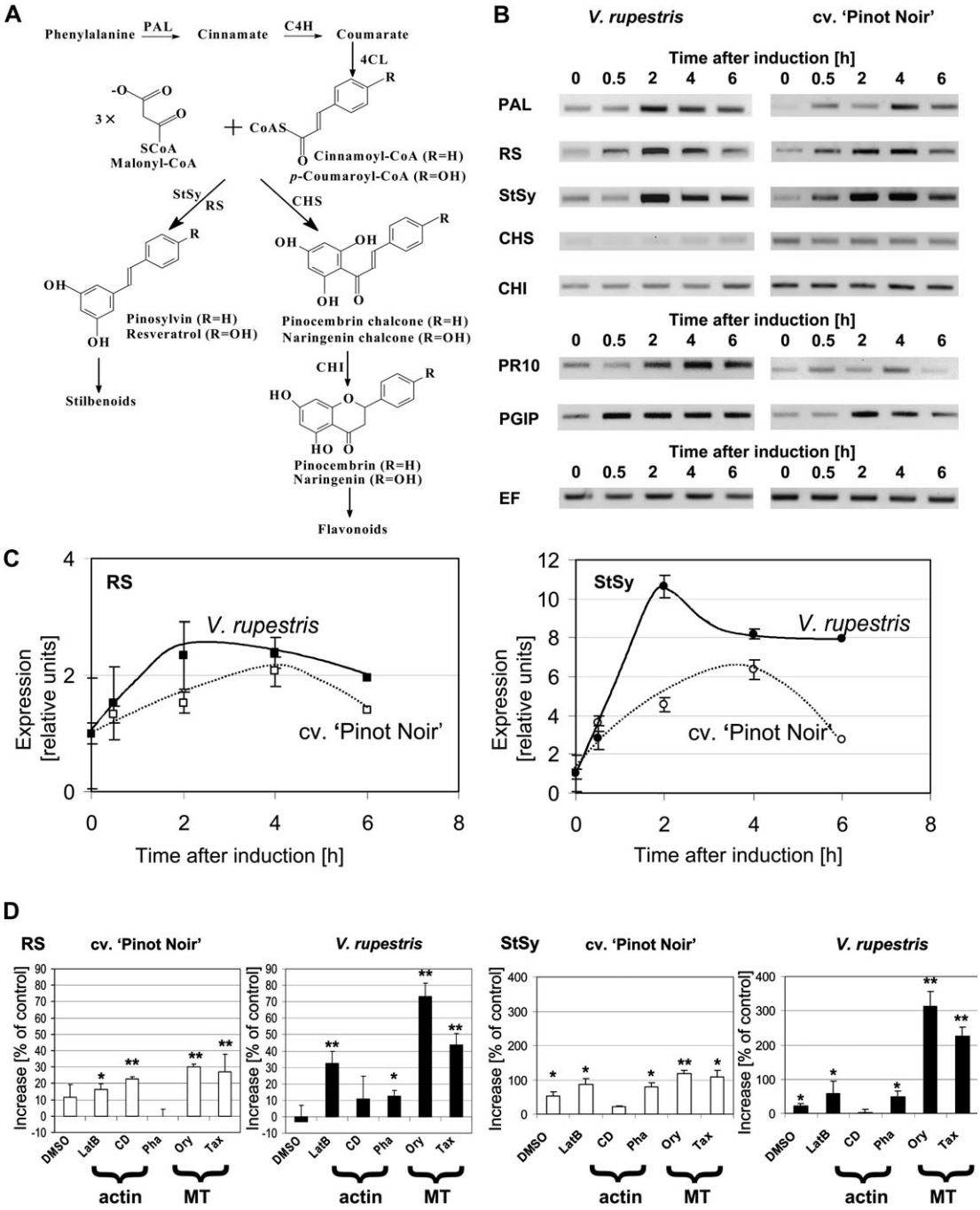

Fig. 4. Response of defence-related genes to Harpin in cv. 'Pinot Noir' and *V. rupestris*. (A) Position of the analysed enzymes in flavonoid and stilbene metabolism. (B) Representative time courses of transcript abundance followed by RT-PCR in response to 9 μg ml^{-1} Harpin. The upper group represents genes of the flavonoid and stilbene pathway: PAL, phenylalanine ammonium lyase; CHS, chalcone synthase; StSy, stilbene synthase; RS, resveratrol synthase; and CHI, chalcone isomerase. The middle group represents pathogenesis-related genes: PR10, pathogenesis-related protein 10; and PGIP, polygalacturonase-inhibiting protein. Elongation factor 1α (EF) was used as internal standard for quantification. (C) Time course of transcript abundance for RS and StSy relative to elongation factor factor 1α. The data represent averages from three independent experimental series; error bars represent standard errors. (D) Expression of RS and StSy relative to untreated controls after pre-treatment with anticytoskeletal compounds for 30 min and allowing the response to be expressed for an additional 2 h. Concentrations were 1 μM for phalloidin (Pha), 1 μM for latrunculin B (LatB), 10 μM for cytochalasin D (CytD), 10 μM for oryzalin (Ory), 10 μM for taxol (Tax), and 1% for DMSO as solvent control for the oryzalin experiment. The data represent averages from three independent experimental series; error bars represent standard errors. * different from the untreated control significant at the 95% confidence level, ** different from the untreated control significant at the 99% confidence level.

was suppressed by dysfunction of the cytoskeleton (Marois *et al.*, 2002). Thus, the present findings on the Harpin elicitor are consistent with an emerging role for microtubules for the defence response to type III effectors.

It is still too early to design clear models for this role of microtubules as triggers/amplifiers of plant defence. Nevertheless, evidence is accumulating that suggests an interaction between microtubules and mechanosensitive ion channels that are important for the induction of defence (Zimmermann *et al.*, 1997; Gus-Mayer *et al.*, 1998). When microtubules were disassembled by antimicrotubule agents, both mechanosensing (Zhou *et al.*, 2007; Wymer *et al.*, 1996) and mechanosensitive calcium fluxes (Ding and Pickard, 1993) were affected. Moreover, the control of protoplast volume during the response to hyperosmotic stress relied on microtubule bundling (so-called macrotubules; Komis *et al.*, 2002). In cold sensing, which probably uses changes of membrane fluidity as a signal, microtubule dynamics were identified as a central component (Abdrakhamanova *et al.*, 2003). Microtubules might act as negative regulators (sphincters) of ion channel activity (in the case of cold sensing) or, in the case of mechanosensing, as stress-focusing elements (susceptors) that collect and convey membrane perturbations to a channel (reviewed in Nick, 2008). In contrast to a sphincter model, stress focusing would be more efficient with stable microtubules, explaining the increased elicitor responsiveness in *V. rupestris* compared with cv. 'Pinot Noir'.

Mechanosensitive calcium channels have been reported to be specifically blocked by lanthanoide ions. The effect of Gd^{3+} ions on Harpin-induced alkalinization was therefore tested as a rapid readout (Supplementary Fig. S2 at *JXB* online), and a dose-dependent progressive inhibition of the pH response in cv. 'Pinot Noir' was observed, which was already manifest at the lowest concentration (20 μM) tested. This Gd^{3+} sensitivity is only slightly lower than the values found from patch–clamp measurements in onion scale epidermis (Ding and Pickard, 1993) and much higher than that reported for other plant tissues, such as adzuki bean hypocotyl (Ikushima and Shimmen, 2005). Interestingly, the alkalinization response in *V. rupestris* was much more reistant to Gd^{3+} inhibition. If one wants to link this difference to the reduced microtubule dynamics in *V. rupestris* as manifest from the higher resistance to oryzalin (Supplementary Fig. S1) and the higher abundance of detyrosinated α-tubulin (Fig. 2G) this would support a role for stable microtubules as negative regulators of the putative calcium channels triggering defence. However, this preliminary evidence for a mechano-susceptor role for microtubules during the induction of plant defence certainly warrants a more thorough investigation in future work.

The finding that not only oryzalin but also taxol can induce the expression of defence genes in the absence of elicitor shows that it is not sufficient for microtubules to be present. In addition, they have to be dynamic in order to fulfil their role in gene expression. This finding is consistent with evidence from other microtubule-dependent signalling responses. For instance, the redistribution of auxin flow by gravitropic stimulation (which is also presumably triggered by stretch-activated ion channels) is blocked not only by microtubule elimination, but also by suppression of microtubule dynamics (rice coleoptiles; Godbolé *et al.*, 2000), cold sensing is elevated in winter wheat cultivars with increased microtubule dynamicity (Abdrakhamanova *et al.*, 2003), cold acclimation is suppressed by taxol in spinach mesophyll (Bartolo and Carter, 1991), and spread of tobacco mosaic virus depends on microtubule dynamics (Ouko *et al.*, 2010).

However, alternative scenarios for the role of the cytoskeleton during induction of defence genes (Fig. 4D) should also be considered. For instance, cytoskeletal disassembly might release transcription factors from retention in the cytoplasm such that they are then translocated into the nucleus and activate expression of their target genes (Chuong *et al.*, 2004; for reviews, see Winder and Ayscough, 2005). In fact, signal-triggered translocation of a transcription factor could be demonstrated for the common plant regulatory factor 2 (CPRF2). This transcription factor is released by activation of phytochromes in parsley cell cultures (Kircher *et al.*, 1999). *In vivo* marker lines for actin filaments and microtubules are presently being generated in the two grapevine cell lines that will help to address this alternative model in the future.

Outlook

Elicitors, which can trigger host resistance, are valuable tools to partially substitute pesticides. The corresponding receptors at the plasma membrane are gradually emerging (Zipfel *et al.*, 2004). Type III secretion effectors that permeate the membrane and enter the cytoplasm would circumvent recognition by plasma membrane-localized receptors. However, since the cytoskeleton seems to be a major target for this type of effector proteins, and since the cytoskeleton acts as a regulator of mechanosensitive ion channels that can trigger plant defence, the intracellular interaction between the effector and cytoskeleton might be sensed by the host cell independently of (or in parallel with) recognition at the plasma membrane. Future work should therefore try to elucidate, on the one hand, the molecular interaction between microtubules and ion channels, and on the other the molecular interaction between type III effectors and the cytoskeleton. To dissect the chain of events, it will be necessary not only to follow cytoskeletal responses *in vivo* using appropriate fluorescent marker lines (to capture also the subtle and rapid changes of microtubules), but also to administer the elicitor to specific locations of the cell to investigate the spatial patterns of cellular responses.

Supplementary data

Supplementary data are available at *JXB* online.

Figure S1. The effect of oryzalin on cell growth. Oryzalin at 1, 10, and 20 μM was added at subcultivation. After 7 d,

the packed cell volume was measured and plotted relative to unchallenged control cells. Error bars represent the SE.

Figure S2. The effect of Gd^{3+} (an inhibitor of stretch-activated ion channels) extracellular alkalization induced by Harpin. The cells were pre-incubated for 30 min with water or different concentrations of $GdCl_3$ before 9 μg ml^{-1} Harpin were added.

Acknowledgements

This work was supported by fellowships of the Chinese Scholarship Council (CSC) to Fei Qiao and Xiaoli Chang. PD Dr Hanns-Heinz Kassemeyer (State Institute of Viticulture, Freiburg) is acknowledged for providing the two grapevine cell cultures, and Sabine Purper for excellent technical assistance during establishment of the cell cultures.

References

Abdrakhamanova A, Wang QY, Khokhlova L, Nick P. 2003. Is microtubule assembly a trigger for cold acclimation? *Plant and Cell Physiology* **44,** 676–686.

Bartolo ME, Carter JV. 1991. Effect of microtubule stabilization on the freezing tolerance of mesophyll cells of spinach. *Plant Physiology* **97,** 182–187.

Belhadj A, Telef N, Saigne C, Cluzet S, Barrieu F, Hamdi S, Mé rillon JM. 2008. Effect of methyl jasmonate in combination with carbohydrates on gene expression of PR proteins, stilbene and anthocyanin accumulation in grapevine cell cultures. *Plant Physiology and Biochemistry* **46,** 493–499.

Chuong SDX, Good AG, Taylor GJ, Freeman MC, Moorhead GBG, Muench DG. 2004. Large-scale identification of tubulin-binding proteins provides insight on subcellular trafficking, metabolic channeling, and signaling in plant cells. *Molecular and Cellular Proteomics* **3,** 970–983.

Coutos-Thévenot P, Poinssot B, Bonomelli A, Yean H, Breda C, Buffard D, Esnault R, Hain R, Boulay M. 2001. *In vitro* tolerance to *Botrytis cinerea* of grapevine 41B rootstock in transgenic plants expressing the stilbene synthase Vst1 gene under the control of a pathogen-inducible PR 10 promotor. *Journal of Experimental Botany* **52,** 901–910.

Dangl JL, Jones JDG. 2001. Plant pathogens and integrated defence responses to infection. *Nature* **411,** 826–833.

Davis KR, Lyon GD, Darvill A, Albersheim P. 1984. Host–pathogen interactions. *Plant Physiology* **74,** 52–60.

Ding JP, Pickard BG. 1993. Mechanosensory calcium-selective cation channels in epidermal cells. *The Plant Journal* **3,** 83–110.

Eggenberger K, Merkulov A, Darbandi M, Nann T, Nick P. 2007. Direct immunofluorescence of plant microtubules based on semiconductor nanocrystals. *Bioconjugate Chemistry* **18,** 1879–1886.

Felix G, Duran J, Volko S, Boller T. 1999. Plants have a sensitive perception system for the most conserved domain of bacterial flagellin. *The Plant Journal* **18,** 265–276.

Felix G, Regenass M, Boller T. 1993. Specific perception of subnanomolar concentrations of chitin fragments by tomato cells: induction of extracellular alkalinization, changes in protein phosphorylation, and establishment of a refractory state. *The Plant Journal* **4,** 307–316.

Godbolé R, Michalke W, Nick P, Hertel R. 2000. Cytoskeletal drugs and gravity-induced lateral auxin transport in rice coleoptiles. *Plant Biology* **2,** 176–181.

Gus-Mayer S, Naton B, Hahlbrock K, Schmelzer E. 1998. Local mechanical stimulation induces components of the pathogen defense response in parsley. *Proceedings of the National Academic of Sciences, USA* **95,** 8398–8403.

Hain R, Reif HJ, Krause E, *et al*. 1993. Disease resistance results from foreign phytoalexin expression in a novel plant. *Nature* **361,** 153–156.

Heath MC. 2000. Nonhost resistance and nonspecific plant defenses. *Current Opinion in Plant Biology* **3,** 315–319.

Higaki T, Goh T, Hayashi T, Kutsuna N, Kadota Y, Hasezawa S, Sano T, Kuchitsu K. 2007. Elicitor-induced cytoskeletal rearrangement relates to vacuolar dynamics and execution of cell death: *in vivo* imaging of hypersensitive cell death in tobacco BY-2 cells. *Plant and Cell Physiology* **48,** 1414–1425.

Hipskind JD, Paiva NL. 2000. Constitutive accumulation of a resveratrol-glucoside in transgenic alfalfa increases resistance to *Phoma medicaginis*. *Molecular Plant-Microbe Interactions* **13,** 551–62.

Ikushima T, Shimmen T. 2005. Mechano-sensitive orientation of cortical microtubules during gravitropism in azuki bean epicotyls. *Journal of Plant Research* **118,** 19–26.

Jabs T, Dietrich RA, Dangl JL. 1996. Initiation of runaway cell death in an *Arabidopsis* mutant by extracellular superoxide. *Science* **273,** 1853–1856.

Jones AM. 2001. Programmed cell death in development and defense. *Plant Physiology* **125,** 94–97.

Jovanović AM, Durst S, Nick P. 2010. Plant cell division is specifically affected by nitrotyrosine. *Journal of Experimental Botany* **61,** 901–909.

Jürges G, Kassemeyer HH, Dürrenberger M, Düggelin M, Nick P. 2009. The mode of interaction between *Vitis* and *Plasmopara viticola* Berk. & Curt. Ex de Bary depends on the host species. *Plant Biology* **11,** 886–898.

Kircher S, Wellmer F, Nick P, Rügner A, Schäfer E, Harter K. 1999. Nuclear import of the parsley bZIP transcription factor CPRF2 is regulated by phytochrome photoreceptors. *Journal of Cell Biology* **144,** 201–211.

Kobayashi I, Kobayashi Y. 2008. Microtubules and pathogen defence. In: Nick P, ed. *Plant cell monographs: plant microtubules*. Berlin: Springer-Verlag, 121–140.

Kobayashi S, Ding CK, Nakamura Y, Nakajima I, Matsumoto R. 2000. Kiwifruit (*Actinidia deliciosa*) transformed with a *Vitis stilbene* synthase gene produce piceid (resveratrol-glucoside). *Plant Cell Reports* **19,** 904–910.

Kobayashi Y, Yamada M, Kobayashi I, Kunoh H. 1997. Actin microfilaments are required for the expression of nonhost resistance in higher plants. *Plant and Cell Physiology* **38,** 725–733.

Komis G, Apostolakos P, Galatis B. 2002. Hyperosmotic stress induces formation of tubulin macrotubules in root-tip cells of *Triticum turgidum*: their probable involvement in protoplast volume control. *Plant and Cell Physiology* **43,** 911–922.

Kortekamp A. 2006. Expression analysis of defence-related genes in grapevine leaves after inoculation with a host and a non-host pathogen. *Plant Physiology and Biochemestry* **44,** 58–67.

Leckband G, Lörz H. 1998. Transformation and expression of a stilbene synthase gene of *Vitis Vinifera* L. in barley and wheat for increased fungal resistance. *Theoretical and Applied Genetics* **96,** 1004–1012.

Maisch J, Nick P. 2007. Actin is involved in auxin-dependent patterning. *Plant Physiology* **143,** 1695–1704.

Marois E, Van den Ackerveken G, Bonas U. 2002. The *Xanthomonas* type III effector protein AvrBs3 modulates plant gene expression and induces cell hypertrophy in the susceptible host. *Molecular Plant-Microbe Interactions* **15,** 637–646.

Morris ER, Walker JC. 2003. Receptor-like protein kinases: the keys to response. *Current Opinion in Plant Biology* **6,** 339–342.

Nick P. 2008. Microtubules as sensors for abiotic stimuli. In: Nick P, ed. *Plant cell monographs: plant microtubules*. Berlin: Springer-Verlag, 175–203.

Nick P, Heuing A, Ehmann B. 2000. Plant chaperonins: a role in microtubule-dependent wall-formation? *Protoplasma* **211,** 234–244.

Nick P, Lambert AM, Vantard M. 1995. A microtubule-associated protein in maize is expressed during phytochrome-induced cell elongation. *The Plant Journal* **8,** 835–844.

Nürnberger T, Brunner F. 2002. Innate immunity in plants and animals: emerging parallels between the recognition of general elicitors and pathogen-associated molecular patterns. *Current Opinion in Plant Biology* **5,** 1–7.

Nürnberger T, Nennstiel D, Jabs T, Sacks WR, Hahlbrock K, Scheel D. 1994. High affinity binding of a fungal oligopeptide elicitor to parsley plasma membranes triggers multiple defense responses. *Cell* **78,** 449–460.

Ouko MO, Sambade A, Brandner K, Ahad A, Heinlein M, Nick P. 2010. Tobacco mutants with reduced microtubule dynamics are less susceptible to TMV. *The Plant Journal* **62,** 829–839.

Reid KE, Olsson N, Schlosser J, Peng F, Lund ST. 2006. An optimized grapevine RNA isolation procedure and statistical determination of reference genes for real-time RT-PCR during berry development. *BMC Plant Biology* **6,** 27–37.

Schmelzer E. 2002. Cell polarization, a crucial process in fungal defence. *Trends in Plant Science* **7,** 411–415.

Seibicke T. 2002. Untersuchungen zur induzierten Resistenz an Vitis spec. PhD thesis. University of Freiburg.

Stark-Lorenzen P, Nelke B, Hänâler G, Mühlbach HP, Thomzik JE. 1997. Transfer of a grapevine stilbene synthase gene to rice (Oryza sativa L.). *Plant Cell Reports* **16,** 668–673.

Stoppin-mellet V, Gaillard J, Vantard M. 2006. Katanin's severing activity favors bundling of cortical microtubules in plants. *The Plant Journal* **46,** 1009–1017.

Szankowski I, Briviba K, Fleschhut J, Schönherr J, Jacobsen HJ, Kiesecker H. 2003. Transformation of apple (Malus domestica Borkh.) with the stilbene synthase gene from grapevine (Vitis vinifera L.) and a PGIP gene from kiwi (Actinidia deliciosa). *Plant Cell Reports* **22,** 141–149.

Takemoto D, Hardham AR. 2004. The cytoskeleton as a regulator and target of biotic interactions in plants. *Plant Physiology* **136,** 3864–3876.

Thordal-Christensen H. 2003. Fresh insights into processes of non host resistance. *Current Opinion in Plant Biology* **6,** 351–357.

Wei ZM, Laby RJ, Zumoff CH, Bauer DW, He SY, Collmer A, Beer SV. 1992*a*. Harpin, elicitor of the hypersensitive response produced by the plant pathogen *Erwinia amylovora*. *Science* **257,** 85–88.

Wei ZM, Sneath BJ, Beer SV. 1992*b*. Expression of *Erwinia amylovora hrp* genes in response to environmental stimuli. *Journal of Bacteriology* **174,** 1875–1882.

Winder SJ, Ayscough KR. 2005. Actin-binding proteins. *Journal of Cell Science* **118,** 651–654.

Wymer C, Wymer SA, Cosgrove DJ, Cyr RJ. 1996. Plant cell growth responds to external forces and the response requires intact microtubules. *Plant Physiology* **110,** 425–430.

Yoshida S, Handa Y, Suzuki T, Ogawa M, Suzuki M, Tamai A, Abe A, Katayama E, Sasakawa C. 2006. Microtubule-severing activity of *Shigella* is pivotal for intercellular spreading. *Science* **314,** 985–989.

Zhao J, Davis LC, Verpoorte R. 2005. Elicitor signal transduction leading to production of plant secondary metabolites. *Biotechnology Advances* **23,** 283–333.

Zhou J, Wang B, Li Y, Wang Y, Zhu L. 2007. Responses of Chrysanthemum cells to mechanical stimulation require intact microtubules and plasma membrane–cell wall adhesion. *Journal of Plant Growth Regulation* **26,** 55–68.

Zimmermann S, Nürnberger T, Frachisse JM, Wirtz W, Guern J, Hedrich R, Scheel D. 1997. Receptor-mediated activation of a plant Ca^{2+}-permeable ion channel involved in pathogen defense. *Proceedings of the National Academic of Sciences, USA* **94,** 2751–2755.

Zipfel C, Robatzek S, Navarro L, Oakeley EJ, Jones JDG, Felix G, Boller T. 2004. Bacterial disease resistance in *Arabidopsis* through flagellin perception. *Nature* **428,** 764–767.